Polymers of intrinsic microporosity containing trifluoromethyl and phenylsulfone groups as materials for membrane gas separation

Du, Naiying; Robertson, Gilles; Song, Jingshe; Pinnau, Ingo; Thomas, Sylvie; Guiver, Michael

Publisher's version / Version de l'éditeur:
https://doi.org/10.1021/ma801858d
Macromolecules, 41, November 24, pp. 9656-9662, 2008

Polymers of Intrinsic Microporosity Containing Trifluoromethyl and Phenylsulfone Groups as Materials for Membrane Gas Separation†

Naiying Du,‡ Gilles P. Robertson,‡ Jingshe Song,‡ Ingo Pinnau,§ Sylvie Thomas,§ and Michael D. Guiver*,‡

Institute for Chemical Process and Environmental Technology, National Research Council of Canada, Ottawa, Ontario K1A 0R6, Canada, and Membrane Technology and Research Inc., 1360 Willow Road, Suite 103, Menlo Park, California 94025-1516

Received August 14, 2008; Revised Manuscript Received October 14, 2008

ABSTRACT: A series of ladder copolymers and a homopolymer were synthesized via aromatic nucleophilic substitution polycondensation of 5,5′,6,6′-tetrahydroxy-3,3,3′,3′-tetramethylspirobisindane with tetrafluoroterephthalonitrile and a new monomer heptafluoro-*p*-tolylphenylsulfone as potential materials for membrane gas separation. Ladder polymers of this type comprising rigid and contorted chain structure have been commonly referred to as polymers of intrinsic microporosity (PIM) on account of their extraordinarily high fractional free volumes (*FFV*) and high gas permeability (*P*). The PIM polymer series of the present study was prepared in high molecular weight and low molecular weight distribution, using new experimental conditions of short reaction times and a high temperature of 160 °C. Polymer chain *d*-spacing was investigated using wide-angle X-ray diffraction. Polymer free volume was calculated from the polymer density and specific van der Waals volume. Gas permeabilities for oxygen and carbon dioxide decreased with increasing content of the trifluoromethylphenylsulfone versus the dinitrile monomer within the copolymer, while the selectivities of gases against nitrogen increased. The pendent phenylsulfone groups likely reside within the interchain free volume of the rigid and contorted ladder polymer, acting to reduce gas permeability and increase selectivity, though with no overall loss of performance relative the Robeson upper bound. Evidence for this is a reduction in *d*-spacing and fractional free volume with increasing content of the trifluoromethylphenylsulfone versus the dinitrile monomer in the copolymer series. The relationship between the gas permeability behavior and structures of the new PIM copolymers is discussed.

Introduction

Polymer membrane gas separation is a dynamic and rapidly growing field of separation technology[1,2] because it can offer a number of advantages, such as low energy use and capital cost.[3] In recent years, much effort has been devoted to the design and preparation of membrane materials whose transport properties are improved by overcoming the "trade-off" behavior between permeability and selectivity.[4−7] Recently a British research group[8−12] reported on some PIMs derived from nitrile monomers whose randomly contorted rigid chains successfully reduce packing efficiency of the macromolecules in the solid state and offer high free volume and high surface areas, which makes them intrinsically microporous materials. Compared to conventional gas separation polymers, the profound significance of these polymers is that they display both very high gas permeability and good selectivity simultaneously, contrary to the normal trade-off behavior of many traditional thermoplastic polymers. These microporous materials are soluble in several common solvents and can be readily fabricated into thin films. Consequently, they have attracted great interest as outstanding membrane materials which have a high potential not only for gas separation, but also for adsorption of small molecules and heterogeneous catalysis. So far, the British group has successfully synthesized several PIM polymers of sufficiently high molecular weight for characterization of films, using a controlled low-temperature aromatic nucleophilic substitution polycondensation of tetraphenol monomers with tetrahalogenated monomers containing nitrile or imine electron-withdrawing groups. Among these polymers, they reported the gas permeability coefficients of some ladder polymers such as PIM-1 and PIM-7 (Scheme 1).

As is well-known, the chemical structure and physical properties of the membrane material influence the permeability and selectivity.[3,13−15] Many studies have shown that an improvement in gas transport properties could be obtained by modifying or tailoring the polymer structure. Considerable attention has been devoted to the preparation of new classes of partially fluorinated polymers because of their unusual properties. Trifluoromethyl groups (−CF_3) have been reported to significantly improve permeability and selectivity by increasing chain stiffness and reducing interchain interactions such as charge-transfer complexes (CTCs).[16,17] In addition, −CF_3 groups

Scheme 1. Preparation and Structures of Polymers PIM-1 and PIM-7

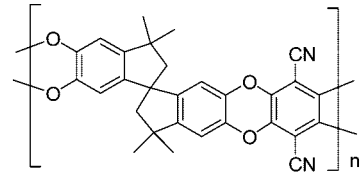

PIM-1

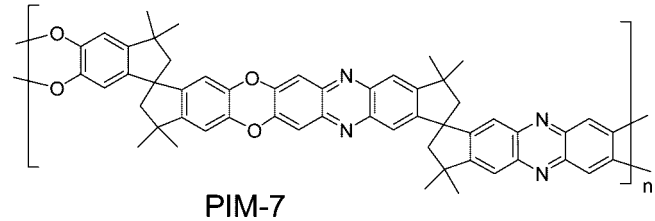

PIM-7

* Corresponding author. E-mail: Michael.guiver@nrc-cnrc.gc.ca.
† NRCC Publication No. 50891.
‡ National Research Council of Canada.
§ Membrane Technology and Research Inc.

10.1021/ma801858d CCC: $40.75
Published on Web 11/14/2008

in a polymer backbone serve several other uses, such as enhancing polymer solubility (commonly referred to as the fluorine effect) without forfeiting thermal stability, giving materials with low dielectric constants and low water absorption, increasing the *FFV* of polymers, and increasing T_g with concomitant decrease and/or elimination of crystallinity. The phenylsulfonyl group ($-SO_2C_6H_5$) is also a useful group which is a common structure employed beneficially in polymers used for gas separation. In general, the $-SO_2-$ group raises T_g and reduces *FFV* and permeability, but with increasing selectivity.[18]

In the present work, a new tetrafluoro monomer containing trifluoromethyl and phenylsulfone groups was synthesized for the preparation of a series of high molecular weight ladder copolymers by copolymerization with different ratios of tetrafluoroterephthalonitrile and tetraphenol monomer 5,5′,6,6′-tetrahydroxy-3,3,3′,3′-tetramethylspirobisindane. In addition, the homopolymer was prepared in high molecular weight from the new monomer. The resulting PIMs had good solubility, attributed to the presence of the $-CF_3$ group; hence, isotropic, dense films could easily be prepared for investigation of their gas permeability properties. The gas permeabilities of the copolymers decrease with increasing content of the phenylsulfone monomer, while gas selectivities against nitrogen decrease, though with no overall reduction in performance relative to the Robeson upper bound. In addition, we report new higher temperature, short reaction time polymerization conditions for producing ladder-type PIMs, which result in high molecular weight polymers with substantially reduced contents of cyclic and cross-linking.

Experimental Section

Materials. 4-Bromo-2,3,5,6-tetrafluorobenzotrifluoride (Matrix Scientific), thiophenol (Aldrich), dimethylacetamide (DMAc, Sigma-Aldrich), sodium hydride (60% dispersion in mineral oil, Sigma-Aldrich), formic acid (Aldrich), hydrogen peroxide solution 30% (w/w) in H_2O (H_2O_2, Aldrich), anhydrous potassium carbonate (K_2CO_3, Sigma-Aldrich), and toluene (Sigma-Aldrich) were used as received. 5,5′,6,6′-Tetrahydroxy-3,3,3′,3′-tetramethylspirobisindane (TTSBI, Sigma-Aldrich) was purified by crystallization from methanol. Tetrafluoroterephthalonitrile (TFTPN, Matrix scientific) was purified by vacuum sublimation at 150 °C under an inert atmosphere.

Characterization Methods. The structures of the polymeric materials were fully characterized using nuclear magnetic resonance (NMR) spectroscopy. NMR analyses were recorded on a Varian Unity Inova spectrometer at a resonance frequency of 399.961 MHz for ^{1}H, 376.276 MHz for ^{19}F, and 100.579 MHz for ^{13}C. ^{1}H and ^{19}F NMR spectra were obtained from samples dissolved in $CDCl_3$ or DMSO-d_6 using a 5 mm pulsed field gradient indirect detection probe. ^{1}H−^{13}C heteronuclear 2D experiments (HSQC, HMBC) were also obtained from the same indirect detection probe. ^{13}C NMR spectra were collected using a 5 mm broadband probe. The solvent signals ($CDCl_3$ ^{1}H 7.25 ppm, ^{13}C 77.00 ppm; DMSO-d_6 ^{1}H 2.50 ppm, ^{13}C 39.43 ppm) were used as the internal references. An external reference was used for ^{19}F NMR: $CFCl_3$ 0 ppm.

Molecular weight and molecular weight distributions were measured by GPC using Ultrastyragel columns and THF as the eluent at a flow rate of 1 mL/min. The values obtained were determined by comparison with a series of polystyrene standards.

Elemental analysis was carried out with a Thermoquest CHNS-O elemental analyzer.

Polymer thermal degradation curves were obtained from thermogravimetric analysis (TGA) (TA Instruments model 2950). Polymer samples for TGA were initially heated to 120 °C under nitrogen gas and maintained at that temperature for 1 h for moisture removal and then heated to 600 at 10 °C/min for degradation temperature measurement. Glass transition temperatures (T_g) were observed from differential scanning calorimetry (DSC) (TA Instruments model 2920), and samples for DSC were heated at 10 °C/min under a nitrogen flow of 50 mL/min and then quenched with liquid nitrogen and reheated at 10 °C/min for the T_g measurement.

Wide-angle X-ray diffraction (WAXD) was used to investigate *d*-spacing. A Bruker AXS GADDS instrument was utilized with Co radiation of wavelength (λ) 1.789 Å. The value of the *d*-spacing was calculated by means of Bragg's law ($d = \lambda/2 \sin \theta$), using θ of the broad peak maximum.

Dense polymer films for gas permeability measurements were prepared from 1−2 wt % polymer solutions in chloroform. Polymer solutions were filtered through 0.45 μm polypropylene filters and then cast into Teflon Petri dishes in a glovebox and allowed to evaporate slowly for 1 day. The films were soaked in methanol and dried in a vacuum oven at 100 °C for 24 h. The resulting membranes with thickness in the range of 50−70 μm were bright yellow and flexible. The absence of residual solvent in the films was confirmed by weight loss tests using TGA.

Permeability coefficients (*P*) of N_2, O_2, and CO_2 were determined at 25 °C with a feed pressure of 50 psig and atmospheric permeate pressure using the constant-pressure/variable-volume method. The permeation flow was measured by a mass flow meter (Agilent ADM 2000). Permeability (*P*) was calculated by using the following equation:

$$P = \left(\frac{273}{T}\right)\left(\frac{dV}{dt}\right)\left(\frac{l}{\Delta pA}\right)$$

where dV/dt is the permeate side flow rate and *T* is the operation temperature (K). The membrane effective area was 9.6 cm^2.

Synthesis. *Preparation of Heptafluoro-p-tolylphenylsulfone (HFTPS).* Into a 50 mL three-necked flask equipped with a magnetic stirrer, an argon inlet, and a condenser, thiophenol (2.42 g, 0.022 mol), NaH (0.88 g, 0.022 mol), and DMAc (5 mL) were added. The mixture was cooled to −20 °C using an ice−salt bath (NaCl/ice = 3:1, w:w) and stirred for 1 h. 4-Bromo-2,3,5,6-tetrafluorobenzotrifluoride (5.94 g, 0.02 mol) in 5 mL of DMAc was added dropwise, and then the temperature was gradually increased to room temperature. After stirring at room temperature for 6 h, the reaction mixture was poured into water, and the crude product was washed three times. The orange color oil was extracted with chloromethane and dried over $MgSO_4$. After removal of chloromethane, the resulting crude heptafluoro-*p*-tolylphenylsulfide was oxidized with formic acid (5 mL) and H_2O_2 (30%) (6 g) at 50 °C for 2 h, resulting in a white-yellow solid sulfone product that was initially purified by chromatography (using 1/1 v/v dichloromethane/hexane). Pure product in the form of white needle crystals was obtained by recrystallization from hexane. Yield: 65%; mp: 134 °C. Elem. Anal. Calcd for $C_{13}H_5F_7O_2S$ (358.23 g/mol): C, 43.95%; H, 1.41%, S 8.95%. Found: C, 43.24%; H, 1.39%; S 8.95%. ^{1}H NMR (chloroform-d): δ 8.09 (d, J = 8.0 Hz, 2H), 7.73 (t, J = 8.0 Hz, 1H), 7.62 (t, J = 8.0 Hz, 2H). ^{19}F NMR (chloroform-d): δ −57.6 (t, J = 22.5 Hz, 3F), −134.3 (m, 2F), −136.9 (m, 2F). ^{13}C NMR (chloroform-d): δ 145.8−143.0 (d, J = 264 Hz), 145.5−142.7 (d, J = 264 Hz), 139.9 (s), 135.3 (s), 129.8 (s), 128.2 (s), 125.3−125.0 (t, J = 14 Hz), 124.1−115.9 (q, J = 275 Hz), 114.2−113.9 (m).

Preparation of PIM-1. A new high-temperature polymerization procedure for PIM-1 is reported here. Into a 100 mL three-necked flask equipped with a magnetic stirrer, an argon inlet, and a Dean−Stark trap, TFTPN (2.001 g, 0.01 mol) and TTSBI (3.404 g, 0.01 mol), anhydrous K_2CO_3 (4.14 g, 0.03 mol), DMAc (20 mL), and toluene (10 mL) were added. During the initial 20−30 min, a small amount of water was observed in the Dean−Stark trap. The mixture was refluxed at 160 °C for 40 min, and then the viscous solution was poured into methanol. A yellow flexible threadlike polymer was obtained. The polymer product was dissolved into chloroform and reprecipitated from methanol. The resulting polymer was refluxed for several hours with deionized water and dried at 100 °C for 48 h.

Preparation of PIM Ladder Polymers Containing Trifluoromethyl and Phenylsulfone Side Groups (TFMPSPIM1−4). A series of TFMPSPIM ladder polymers 1−4 were synthesized by polycondensation of TTSBI, HFTPS, and TFTPN (with the molar ratio 1:1:0; 3:2:1; 2:1:1; 3:1:2) using a new

Scheme 2. Synthetic Route to the TFMPSPIM

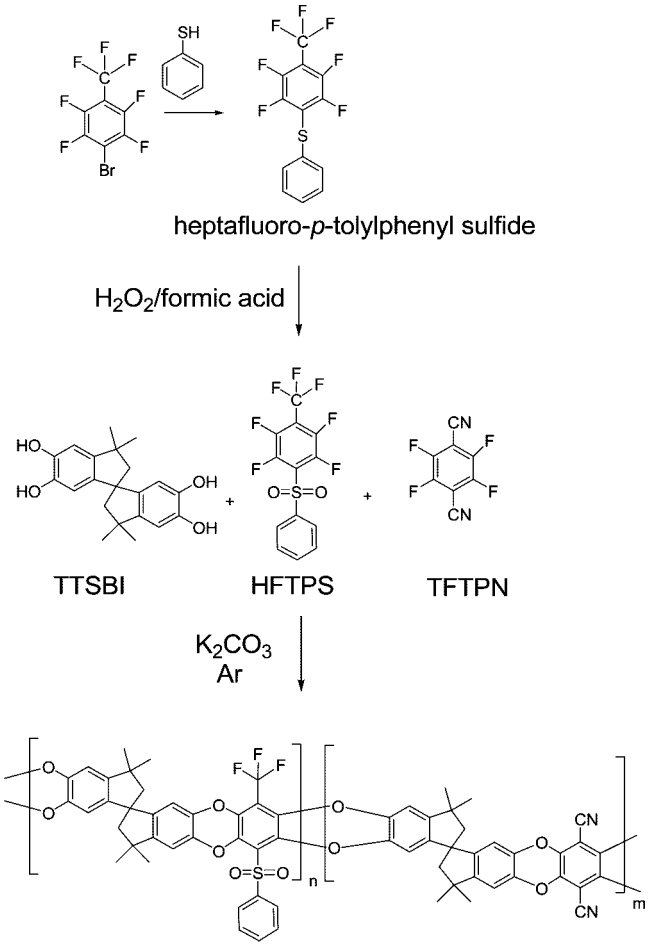

procedure similar to that of PIM-1 above. ^{19}F NMR (chloroform-d): −56.2 ppm (s, 3F).

Results and Discussion

Monomer Synthesis. Alsop et al. previously reported the synthesis of HFTPS by oxidation of heptafluoro-*p*-tolylphenylsulfide, obtained from the reaction of thiophenol with octafluorotoluene.[19] As far as we are aware, HFTPS has not previously been utilized as a monomer in a polymerization reaction. The present synthetic method is different from the previous report and comprises two steps as shown in Scheme 2. In the first step, the bromine atom in 4-bromo-2,3,5,6-tetrafluorobenzotrifluoride is displaced by thiophenol using NaH at −20 °C. Both F−Ar and Br−Ar react with thiophenols under basic conditions by aromatic nucleophilic substitution reaction, but the reactivity is different. At higher temperatures, F−Ar is more reactive, while at lower temperatures, Br−Ar is more easily displaced, since −Br is an efficient leaving group specifically for reactions with thiophenolates. Elevated temperatures (above 60 °C) or longer reaction times would lead to more byproducts, indicating that the comparative selectivity of thiophenol group decreases. K_2CO_3 can be also used as a base for this reaction at these conditions. However, at lower temperatures, water cannot be removed, and it continues to react with Ar−F to form Ar−OH, thereby reducing the yield. A small amount of CaH_2 was added to the reaction at the beginning to eliminate the water efficiently. Although the resulting $Ca(OH)_2$ is basic, it does not react readily with F−Ar at low temperature due to the poor solubility. The crude product was oxidized without purification. The thioether could be completely converted to sulfone using excess H_2O_2 in a heterogeneous formic acid suspension at 50 °C within 2 h. In terms of its use as a monomer for ladder polymers, the new monomer relies on the electron-withdrawing power of sulfone, rather than nitrile used in the synthesis of PIM-1.

Polymerization. The ladder PIMs (including TFMPSPIM and PIM-1) containing $-CF_3$, $-SO_2C_6H_5$, and −CN groups were synthesized by S_NAr polycondensation using various feed ratios of TTSBI/HFTPS/TFTPN, so that polymers with different molar percentages of −CN and $-CF_3/-SO_2C_6H_5$ (Scheme 2) were obtained. The ideal structures of the ladder polymers are linear chains without cross-linking. The characterization results are listed in Table 1. The polymers are named TFMPSPIM1−4, where PIM stands for polymer of intrinsic microporosity; TFM and PS refer to trifluoromethyl and phenylsulfonyl, respectively.

The synthesis of ladder polymers with substantially reduced amounts of cyclic species or cross-linking was accomplished using new polymerization conditions applied to PIMs. A higher polymerization temperature of 160 °C and higher monomer concentrations (monomer:solvent = 1 mmol:2 mL) in DMAc were used compared with the previously reported polymerization conditions conducted at lower temperatures. DMAc is largely compatible with both the monomer salts and growing polymer chain at this temperature. In addition, excess toluene (toluene: DMAc = 4: 1 v/v) was introduced into the reaction not only to remove generated water but also to provide solubility enhancement of the polymer. In a similar reaction carried out in the absence of excess toluene, cross-linked polymer formed readily in the latter stages of polymerization (approximately the last 10 min). The new high-temperature polymerization procedure for PIM-1 reported here led to high molecular weight polymers within 40 min. Compared with the originally reported PIM synthesis,[9] the reaction conditions reported here require less time and the explosion-like polycondensation is relatively easy to control. In contrast with typical nucleophilic aromatic substitution polycondensation reaction to produce poly(aryl ether)s, the formation of the ladder polymers is more complicated. As shown in Schemes 1 and 2, each monomer has four reactive groups, greatly increasing the susceptibility for cross-linking to occur. However, using the present reaction conditions, GPC results (Table 1) show that high molecular weight polymers (M_n > 55 000 Da) were obtained and the polydispersity index is ∼2.0, which is consistent with the results of typical polycondensation reactions in which each monomer has two reactive sites. On GPC curves (Figure 3), there is no shoulder peak in the low or high molecular weight region around the main peak, indicating that it is a clean reaction with few cross-linked or cyclic structures. GPC results also showed that TFMPSPIM1−4 polymers with higher molecular weight as compared to PIM-1

Table 1. Physical Properties of TFMPSPIM1−4 and PIM-1

polymers	TTSBI (molar ratio)	HFTPS (molar ratio)	TFTPN (molar ratio)	M_n	M_w	M_w/M_n	tensile stress at break (MPa)	tensile strain at break (%)
TFMPSPIM1	1	1	0	77 000	156 000	2.0	33.6	3.9
TFMPSPIM2	3	2	1	71 000	143 000	2.0	38.3	4.4
TFMPSPIM3	2	1	1	66 000	139 000	2.1	43.3	5.2
TFMPSPIM4	3	1	2	64 000	110 000	1.7	46.2	5.6
PIM-1	1	0	1	55 000	85 000	1.6	47.1	11.2

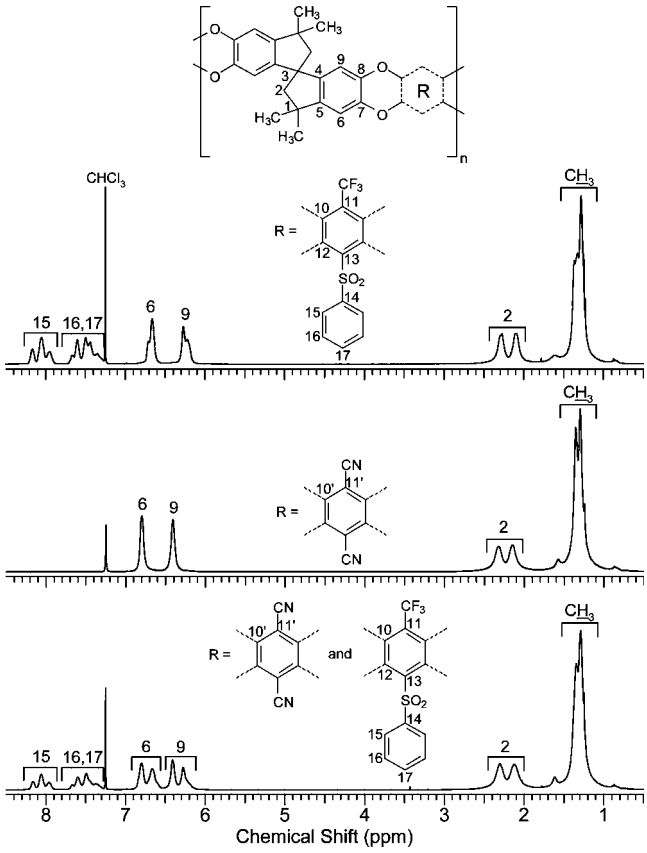

Figure 1. [1]H NMR spectra of TFMPSPIM1, TFMPSPIM3, and PIM-1.

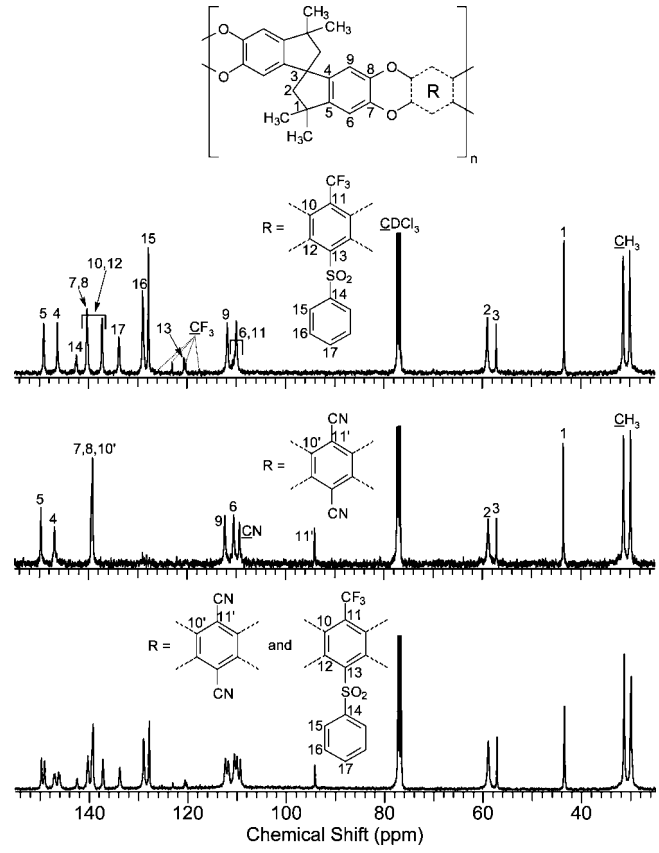

Figure 2. [13]C NMR spectra of TFMPSPIM1, TFMPSPIM3, and PIM-1.

were obtained under the same reaction condition. The M_n of the polymer decreased as the ratio of monomer HFTPS in the copolymer was reduced. The homopolymer prepared from HFTPS had the highest M_n, while PIM-1 homopolymer had the lowest. A plausible explanation is that the $-CF_3$ group and $-SO_2C_6H_5$ enhance the solubility of the polymer and growing chain, so that the polymer chains are unfolded, uncoiled, and unpacked, and the chain-growth step reaction is facilitated. Meanwhile, the −F and −OH on neighboring aromatic rings readily react with each other and form ladder structures with less propensity for cross-linking.

The mechanical properties of the ladder polymer series are listed in Table 1. Tensile stress at break and tensile strain at break decreased due to the introduction of increasing amounts of $-CF_3$ and $-SO_2C_6H_5$ into the polymer chain. In the series from PIM 1 to TFMPSPIM-4, tensile strain at break drops off sharply from 11.2% to 5.6% while almost maintaining the same tensile stress at break (from 47.1 to 46.2 M Pa), which implies that the polymer had additional rigidity due to the introduction of pendant $-CF_3$ and $-SO_2C_6H_5$ groups.

NMR Analysis. The TFMPSPIM1 and PIM-1 homopolymers and TFMPSPIM2−4 copolymers were fully characterized by [1]H, [13]C, and [19]F NMR spectroscopy. Carbon NMR was particularly useful as there are many quaternary carbon atoms on these polymers. Stacked [1]H NMR spectra of TFMPSPIM1, PIM-1, and TFMPSPIM3 are displayed in Figure 1 while [13]C spectra of the same polymer series are displayed in Figure 2. The aliphatic and aromatic hydrogen signals of PIM-1 and TFMPSPIM1 were unambiguously assigned with the help of 2D HSQC and HMBC. Long-range C−H correlations involving C1 with C$\underline{H}_3$ (^{2}JC−C−H) and H6 (^{3}JC−C−C−H) helped differentiate the H6 signal from H9. Most PIM-1 carbon signals were assigned using direct HSQC C−H couplings. All the quaternary carbon atom signals from the TTSBI monomer

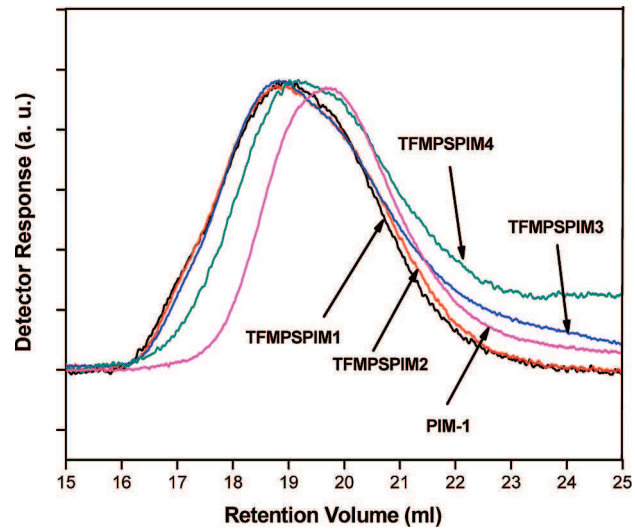

Figure 3. GPC curves for TFMPSPIM1−4 and PIM-1.

residue were identified by multiple bonds C−H correlations (HMBC) with previously assigned proton frequencies. The absence of hydrogen atoms on the TFTPN monomer results in no signals in 2D HSQC and HMBC NMR. Therefore, C10′, C11′, and −CN were assigned on the basis of their chemical shifts. C10′ is strongly deshielded by the electronegative oxygen atom and was therefore easily assigned as the signal at the highest frequency (139 ppm). On the other hand, C11′ is shielded by the electron-donating effect through delocalization of the same oxygen atoms. C11′ is sandwiched between two C−O groups and will therefore be strongly shielded and shifted to very low frequencies; hence the peak at 94 ppm. The last quaternary carbon, −CN, appears in the typical −CN range (109

Table 2. Thermal Properties of the Polymers

polymers	T_d (°C)[a]	T_d (°C)[b]	T_{d5} (°C)[c]	RW (%)[d]
TFMPSPIM1	352.8	430.3	437.7	59.15
TFMPSPIM2	357.6	450.9	458.5	62.82
TFMPSPIM3	368.3	463.5	468.3	63.04
TFMPSPIM4	370.9	482.8	486.8	64.79
PIM-1	429.6	492.6	495.4	68.17

[a] Actual onset temperature of decomposition. [b] Extrapolated onset temperature of decomposition measured by TGA. [c] Five percent weight loss temperature measured by TGA. [d] Residue weight at 600 °C under N_2.

ppm). A ^{13}C NMR prediction spectrum was obtained (ACD Laboratories prediction software, v. 10.04, Dec 2006) in order to compare the actual and predicted chemical shifts for C10′, C11′, and CN. The predicted chemical shifts were within 2 ppm for C10′ and C11′ and within 7 ppm for CN, hence validating our peak assignments based on NMR knowledge. The ^1H and ^{13}C NMR spectra of TFMPSPIM1 homopolymer were obviously similar to those of PIM-1 homopolymer due to their identical TTSBI monomer residue within the backbone. The additional signals arising from the new monomer were readily assigned in both ^1H and ^{13}C NMR with the help of 2D HMBC and HSQC. As before, the C−O carbon atoms C10′ and C12′ were assigned to high frequencies (137−141 ppm). The $-CF_3$ and C11′ were identified by their spin-couplings with the ^{19}F atoms ($^1JC-F = 277$ Hz, $^2JC11'-F \approx 30$ Hz). The ^1H and ^{13}C NMR spectra of the copolymer TFMPSPIM3 prepared from the monomer ratio 2 TTSBI:1 HFTPS:1 TFTPN are shown as the lower spectra in Figures 1 and 2. As expected, these spectra display the same characteristics as the two fully characterized homopolymers PIM-1 and TFMPSPIM1. The specific low-frequency (94 ppm) C11′ of PIM-1 and the specific quartet $-\underline{C}F_3$ of TFMPSPIM1 are clearly visible in the ^{13}C NMR spectrum. Furthermore, the experimental ratio of intensity values for proton H-15, 16, 17 compared with H-6, 9 is exactly 5H:8H, as expected for two repeat units of the TFMPSPIM3 copolymer. Finally, the ^{19}F NMR spectra (not shown) were collected for all three polymers. Only TFMPSPIM1 and TFMPSPIM3 showed a signal at ca. 56 ppm which is characteristic of a $-C\underline{F}_3$ group. It is worthwhile mentioning that no aromatic F signal was observed.

Thermal Analysis. Thermal analyses for TFMPSPIM and PIM-1 were carried out, and the results are summarized in Table 2. All the polymers have no discernible T_g in the measured range of 50−350 °C. TGA experiments showed that all the polymers have excellent thermal stabilities, and the actual onset temperature of decomposition in nitrogen is above 350 °C. There is also some trend between this temperature and monomer ratio. Generally, nitrile-containing polymers have high thermal stability, likely due to strong dipolar interactions. Table 2 shows that with increasing molar content of −CN in the polymers the onset of thermal decomposition also increased. However, TFMPSPIM homopolymer and copolymers all showed very good thermal stability even after the replacement of nitrile with $-CF_3$ and pendant $-SO_2C_6H_5$ groups.

X-ray Diffraction Studies. The disruption in chain packing is validated by *FFV* and was calculated using the following relationship:[20]

$$V_f = (V_{sp} - 1.3V_w)$$

$$FFV = V_f/V_{sp}$$

where V_f is the free volume and V_{sp} is the specific volume. Membrane samples had a density in the range 1.06−1.21 g cm^{-3}, as determined by measurements of their weight in air and in ethanol. V_w is the specific van der Waals volume calculated using the group contribution method of Bondi.[21,22]

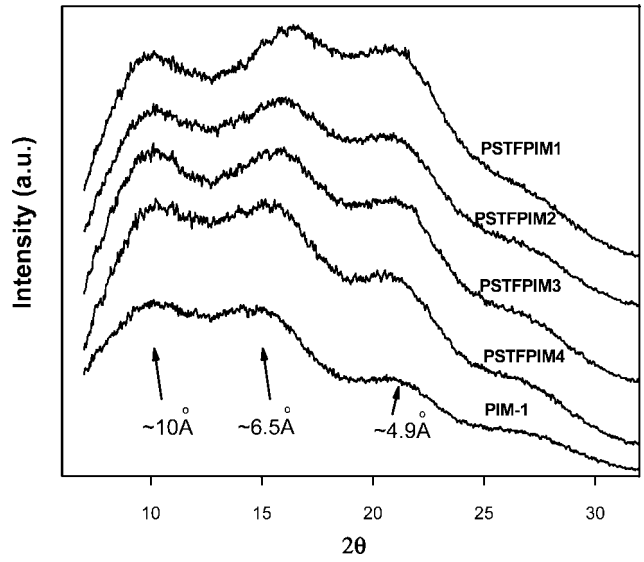

Figure 4. WAXD of TFMPSPIM1−4 and PIM-1.

FFV increased with increasing nitrile content, suggesting that TFMPSPIMs with increasing $-CF_3$ and $-SO_2C_6H_5$ pendant groups pack interchain space more efficiently than PIM-1, as shown in Table 3.

These assumptions are supported by the X-ray diffraction measurements shown in Figure 4, which reveal that all the polymers were amorphous. Three broad peaks were observed for all polymers. The peak at higher angles (4.9 Å) can be attributed to the chain-to-chain distance of space efficiently packed chains. The second peak, corresponding to more loosely packed polymer chains with a *d*-spacing of ∼6.50 Å, is attributed to polymers maintaining their conformation with micropores between the chains.[23] The exact *d*-spacing values were calculated from WAXD spectra by Bragg's law and are listed in Table 3. These values are consistent with the explanation of the free volume theory. The *d*-spacing of TFMPSPIM1 homopolymer is about 6.30 Å, and it becomes larger with decreasing molar amounts of $-CF_3$ and $-SO_2C_6H_5$ groups in the main chain, suggesting that the $-CF_3$ and $-SO_2C_6H_5$ pendant groups affect the polymer chain packing and decrease polymer *d*-spacing, possibly by interchain space filling. The third peak at a *d*-spacing of ∼10 Å corresponds to the distance between the spiro-carbon atoms, which is ∼10−15 Å for PIM-1 and is very similar to the calculated distances for TFMPSPIM1−4. The significance of the distance between the spiro-carbon centers is that the relatively planar rigid chain segments change direction and are skewed at these points, preventing efficient chain packing.

Pure-Gas Permeation Properties. A trade-off relationship is usually observed between permeability (*P*) and ideal selectivity (α) for common gases in glassy or rubbery polymers; i.e., higher permeability is gained at the cost of lower selectivity and vice versa. Upper bound performance lines for the relationship between gas permeability and selectivity have been proposed by Robeson.[6] Pure-gas permeability coefficients (*P*) were measured on dense films (PIM-1, TFMPSPIM1−4) for O_2, N_2, and CO_2, and a summary of these *P* values and ideal selectivities for various gas pairs is shown in Table 4. As can be seen in Table 4, TFMPSPIM1−4 were significantly more selective than PIM-1 for all gases.

Although the permeability of O_2 is reduced with increasing amounts of $-CF_3$ and $-SO_2C_6H_5$ groups, TFMPSPIM1−4 permeability/selectivity data points are all above the upper bound line reported by Robeson, as shown in Figure 5.

Table 3. Physical Properties of TFMPSPIM1-4 and PIM-1

polymers	*d*-space (Å)	ρ (g/cm^3)	V_{sp} (cm^3/g)	*M* (g/mol)	V_w (cm^3/mol)	V_f (cm^3/g)	*FFV*
TFMPSPIM1	6.30	1.214	0.82	618.62	304.4	0.180	0.22
TFMPSPIM2	6.34	1.196	0.84	565.90	285.0	0.185	0.22
TFMPSPIM3	6.50	1.156	0.87	539.55	275.4	0.206	0.24
TFMPSPIM4	6.60	1.089	0.91	513.20	265.7	0.237	0.26
PIM-1	6.88	1.063	0.94	460.48	246.3	0.244	0.26

Table 4. Gas Permeabilities and Ideal Selectivities of TFMPSPIM1-4 and PIM-1

	P (barrer[a])		selectivity α[b]		
polymers	O_2	N_2	CO_2	O_2/N_2	CO_2/N_2
TFMPSPIM1	156	33	731	4.7	22
TFMPSPIM2	308	75	1476	4.1	20
TFMPSPIM3	561	158	2841	3.6	18
TFMPSPIM4	737	217	3616	3.4	17
PIM-1	1133	353	5366	3.2	15
PIM-1[11]	370	92	2300	4.0	25
PIM-1[24]	786	238	3496	3.3	15

[a] Permeability coefficients measured at 25 °C and 50 psig feed pressure. 1 barrer = 10^{-10} [cm^3 (STP) cm]/(cm^2 s cmHg). [b] Ideal selectivity $\alpha = (P_a)/(P_b)$.

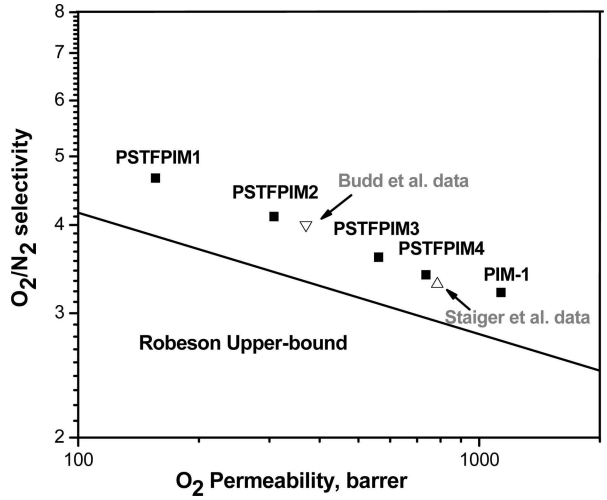

Figure 5. Trade-off between O_2 permeability and O_2/N_2 selectivity of PIM-1 and TFMPSPIM1−4 membranes relative to the Robeson upper bound line. ▽ is data from Budd et al., which are for measurements reported at 200 mbar (2.9 psia) feed pressure at 30 °C.[11] △ is data from Staiger et al., which are for measurements reported at 4 atm (58.8 psia) feed pressure at 35 °C.[24]

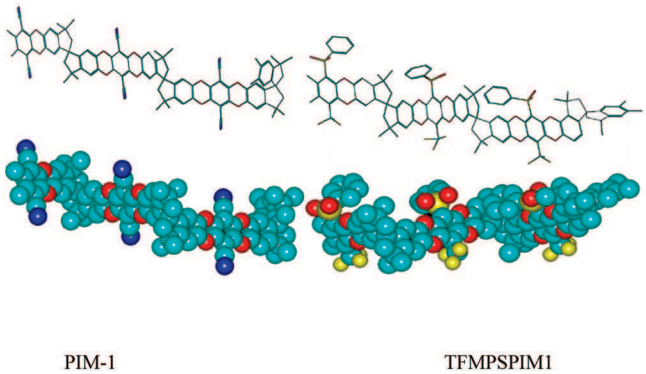

Figure 6. Models of the PIM-1 and TFMPSPIM1 as calculated with energy minimization by HyperChem software.

In comparison with PIM-1, which was tested under the same conditions, TFMPSPIM1−4 have significantly higher O_2/N_2 and CO_2/N_2 selectivity. From a material and structural viewpoint, smaller interchain distance coupled with chain rigidity imparts increased selectivity but lower permeability, whereas greater interchain distance imparts higher permeability but lower selectivity. The $-CF_3$ and $-SO_2C_6H_5$ groups in TFMPSPIM1−4 are hidden within the spirocyclic main chain structure, which maintains its zigzag conformation. While these pendant groups do not increase *FFV*, they increase chain stiffness and likely have an effect of interchain space filling. The ▽ and △ symbols in Figure 5 show previous gas permeability data reported by Budd et al. and Staiger et al., respectively, for PIM-1.[11,24] Compared to data reported by Budd et al. for films cast from tetrahydrofuran and measured at low gas feed pressure, the pure-gas oxygen permeability of PIM-1 reported in our work (∼1133 barrer) is about 3 times higher, but with a reduction in oxygen/nitrogen selectivity from 4 to 3.2 (Table 4). However, our data are more consistent with that of Staiger et al.; the pure-gas permeabilities and selectivities of a PIM-1 film made from methylene chloride are similar to our data for a chloroform-solution-cast PIM-1 film. This result is not surprising as the gas permeation properties of highly rigid glassy polymers depend strongly on film formation protocols, such as casting solvent type and drying conditions.[25]

Molecular Modeling. Conformational analysis of TFMPSPIM1 and PIM-1 was modeled with three repeat unit lengths to study the effect and distribution of $-CF_3$ and $-SO_2C_6H_5$ on chain geometry and steric interaction. The calculation results of geometry optimization with energy minimization using the AMBER method provides a visualization of major conformational changes occurring in the polymers, as shown in Figure 6. The chains of PIM-1 homopolymer containing −CN side groups, shown for comparison, have a relatively spiro-zigzag linear and regular ladder structure, which would lead to less chain packing. Compared with PIM-1, TFMPSPIM1 homopolymer showed a similarly unperturbed coil conformation. Although $-CF_3$ and $-SO_2C_6H_5$ are more bulky than the −CN group, they do not change the spiro-zigzag ladder chain. In addition, the rigidity of the ladder polymer chain with $-CF_3$ and $-SO_2C_6H_5$ groups can be enhanced by hindering bond distortion within the ladder chain; hence, selective diffusion ability can be improved. Presumably, the pendant phenylsulfonyl group resides within the interchain free volume and also acts to reduce permeability, while increasing selectivity. This is in good agreement with our gas permeation results. The molecular modeling result may help to explain why, as compared to PIM-1, the co-effects of TFMPSPIM improve their gas selectivity without overall loss of performance relative to the upper bound line.

Conclusions

New ladder PIMs (TFMPSPIM1−4) with high molecular weight and low polydispersity, exhibiting intrinsic microporosity, were synthesized under experimental conditions previously unreported for this class of materials. Elevated reaction temperature and short reaction times (within 1 h) led to high molecular weight PIMs, extending the possible structures beyond those reported previously. The newly reported high-temperature polymerization conditions for this class of ladder polymers were effective in largely avoiding cross-linking and cyclic structures, due to enhancement in the solubility of monomer salt and polymer by using high-temperature, high-concentration conditions. In addition, the presence of $-CF_3$ and $-SO_2C_6H_5$ side

groups acts favorably to increase polymer solubility. While all these ladder polymers have high T_d, the thermal properties decreased with respect to PIM-1, with increasing molar ratios of $-CF_3$ and $-SO_2C_6H_5$ in the TFMPSPIM. These polymers exhibit intrinsic microporosity, which was supported by X-ray diffraction measurements, gas permeability measurements, and molecular modeling. The TFMPSPIM1−4 series were significantly more selective to all gases than PIM-1. They exhibit high selectivity coupled with a permeability that combines to exceed the Robeson upper bound for O_2/N_2. This performance is attributed to introduction of the side groups, which boost selectivity while maintaining good permeability. These results suggest that the $-CF_3$ and $-SO_2C_6H_5$ groups on the polymer main chains exert a considerable influence on the gas transport properties.

Acknowledgment. This work was supported primarily by the Climate Change Technology and Innovation Initiative, Greenhouse Gas project (CCTII, GHG). Partial support was also provided by the U.S. Department of Energy (SBIR Contract DE-FG02-05ER84243). The authors are grateful to Dr. Pamela Whitfield of the National Research Council for the WAXD measurements.

References and Notes

(1) Stern, S. A. *J. Membr. Sci.* **1994**, *94*, 1–65.
(2) Maier, G. *Angew. Chem., Int. Ed.* **1998**, *37*, 2960–2974.
(3) Pandey, P.; Chauhan, R. S. *Prog. Polym. Sci.* **2001**, *26*, 853–893.
(4) Kim, T. H.; Koros, W. J.; Husk, G. R.; O'Brien, K. C. *J. Membr. Sci.* **1988**, *37*, 45–62.
(5) Lee, C. L.; Chapman, H. L.; Cifuentes, M. E.; Lee, K. M.; Merrill, L. D.; Ulman, K. L.; Venkataraman, K. *J. Membr. Sci.* **1988**, *38*, 55–70.
(6) Robeson, L. M. *J. Membr. Sci.* **1991**, *62*, 165–185.
(7) Robeson, L. M.; Burgoyne, W. F.; Langsam, M.; Savoca, A. C.; Tien, C. F. *Polymer.* **1994**, *35*, 4970–4978.
(8) Budd, P. M.; Ghanem, B. S.; Makhseed, S.; McKeown, N. B.; Msayeb, K. J.; Tattershall, C. E. *Chem. Commun.* **2004**, 230–231.
(9) Budd, P. M.; Elabas, E. S.; Ghanem, B. S.; Makhseed, S.; McKeown, N. B.; Msayeb, K. J.; Tattershall, C. E.; Wong, D. *Adv. Mater.* **2004**, *16*, 456–459.
(10) Budd, P. M.; McKeown, N. B.; Fritsch, D. *J. Mater. Chem.* **2005**, *15*, 1977–1986.
(11) Budd, P. M.; Msayeb, K. J.; Tattershall, C. E.; Reynolds, K. J.; McKeown, N. B.; Fritsch, D. *J. Membr. Sci.* **2005**, *251*, 263–269.
(12) McKeown, N. B.; Budd, P. M.; Msayeb, K. J.; Ghanem, B. S.; Kingston, H. J.; Tattershall, C. E.; Makhseed, S.; Reynolds, K. J.; Fritsch, D. *Chem.—Eur. J.* **2005**, *11*, 2610–2620.
(13) Aoki, T. *Prog. Polym. Sci.* **1999**, *24*, 951–993.
(14) Dai, Y.; Guiver, M. D.; Robertson, G. P.; Kang, Y. S.; Lee, K. J.; Jho, J. Y. *Macromolecules* **2004**, *37*, 1403–1410.
(15) George, S. C.; Thomas, S. *Prog. Polym. Sci.* **2001**, *26*, 985–1017.
(16) Banerjee, S.; Maier, G.; Burger, M. *Macromolecules* **1999**, *32*, 4279–4289.
(17) Dai, Y.; Guiver, M. D.; Robertson, G. P.; Kang, Y. S. *Macromolecules* **2005**, *38*, 9670–9678.
(18) Paul, D. R.; Yampol'ski, Y. In *Polymeric Gas Separation Membranes*; CRC Press: London, 1994; p 107.
(19) Alsop, D. J.; Burdon, J.; Tatlow, J. C. *J. Chem. Soc.* **1962**, 1801–1805.
(20) Lee, W. M. *Polym. Eng. Sci.* **1980**, *20*, 65–79.
(21) Bondi, A. *J. Phys. Chem.* **1964**, *68*, 441–451.
(22) van Krevelen, D. W. In *Properties of Polymers: Their Correlation with Chemical Structure; Their Numerical Estimation and Prediction from Additive Group Contributions*; Elsevier: Amsterdam, The Netherlands, 1990.
(23) Weber, J.; Su, Q.; Antonietti, M.; Thomas, A. *Macromol. Rapid Commun.* **2007**, *28*, 1871–1876.
(24) Staiger, C. L.; Pas, S. J.; Hill, A. J.; Cornelius, C. *J. Chem. Mater.* **2008**, *20*, 2606–2608.
(25) Moe, M. B.; Koros, W. J.; Hoehn, H. H.; Husk, G. R. *J. Appl. Polym. Sci.* **1988**, *36*, 1833–1846.

MA801858D